

Progression of malaria induced pathogenicity during chloroquine therapy

Zaid, O.I.^{1*}, Abd. Majid, R.², Sidek, H.M.³, Noor, S.M.⁴, Abd Rachman-Isnadi, M.F.⁵, Bello, R.O.⁵, Chin, V.K.⁵ and Basir, R.^{5*}

¹Pharmacology Unit, Department of Pharmacy, Al Rafidain University, Al Mustansyria, Baghdad, Iraq

²Department of Medical Microbiology and Parasitology, Faculty of Medicine and Health Sciences, Universiti Putra Malaysia, 43400, Serdang, Selangor

³School of Bioscience and Biotechnology, Faculty of Science and Technology, Universiti Kebangsaan Malaysia, 43600 UKM Bangi, Selangor, Malaysia

⁴Department of Pathology, Faculty of Medicine and Health Sciences, Universiti Putra Malaysia, 43400, Serdang, Selangor

⁵Department of Human Anatomy, Faculty of Medicine and Health Sciences, Universiti Putra Malaysia, 43400, Serdang, Selangor

*Corresponding author e-mails: rusliza@upm.edu.my (R. Basir), Zaid.2002.205@gmail.com (Zaid O Ibraheem)

Received 2 April 2019; received in revised form 18 October 2019; accepted 21 October 2019

Abstract. Treatment Failure with chloroquine is one of the challenges that faced the dedicated efforts to eradicate malaria. This study aims at investigating the impact of treatment failure with chloroquine on the progression of the disease-induced histo-pathogenic and immunogenic outcomes. To achieve this, Rane's protocol with modifications was applied on a model of *Plasmodium berghei* ANKA infected ICR mice to determine the dose response curve of chloroquine and to screen the treatment impact on the disease progression. Chloroquine was given at 1, 5, 10, 15 and 20 mg/kg once the parasitemia reached to 20-30% (the experimental initiation point). During the subsequent days, the mice were monitored for changes in the clinical signs, hematology parameters and the progress of the parasitemia until the parasitemia reached to 60-70% (the experimental termination point) or up to 10 days after chloroquine administration in case of achieving a complete eradication of the parasite. At the end, the mice were exsanguinated and their blood and organs were collected for the biochemistry and the histology study. A complete eradication of the parasite was achieved at 20 mg/kg while recrudescence was observed at the lower doses. At 1 mg/kg, the parasite growth was comparable to that of the positive control. The histo-pathogenic and immunogenic changes were stronger in the groups that experienced recrudescence (at 5 and 10 mg/kg). All in all, the study highlights the possibility of having a worsened clinical condition when chloroquine is given at its sub-therapeutic doses during malaria treatment.

INTRODUCTION

Malaria is a devastating multi-organs infectious disease afflicting millions of people and claiming the life of other thousands around the world. It induces metabolic derangements, hematologic disarrays as well as degenerative and inflammatory changes in different organs (De Souza *et al.*, 2010; Basir *et al.*, 2012).

Treatment failure with chloroquine is one of the major catastrophes in the realm of

malaria chemotherapy. Chloroquine is the most indispensable antimalarials due to its cost-effectivity, strong potency and relative safety as compared to the others. But, unfortunately, it started to lose its token due to the emergence of resistance among different strains of the parasite and due to factors related to its pharmacokinetic characters. Chloroquine tends to deposit in the lean body mass especially in liver or skin failing its access to its target site of action (Ono, Yamada M *et al.*, 2003). Previous

studies revealed wide interindividual variations in the pharmacokinetic characters of chloroquine and proposed a difficulty in maintaining its serum level within the therapeutic limit. In spite of all of these challenges, chloroquine is used inevitably in the poor endemic areas of malaria due to economic factors (McLachlan *et al.*, 1993). This urged the health authorities to search for other alternatives or take measures to downsize the unwanted consequences of its treatment failure.

This study aimed at screening the impact of chloroquine treatment failure on the progression of the disease induced pathogenic events using an experimental model of chloroquine treated *Plasmodium berghei* ANKA infected ICR mice.

METHODOLOGY

1. Animals

Imprint Control Region (ICR) mice; weighing (17-20 g), were procured from Takrif Bistari Enterprise/ Kuala Lumpur/ Malaysia. They were reared in the transient room facility of the Faculty of Medicine and Health Sciences/ University Putra Malaysia, with free access to the standard rodents' chow and drinking water (*ad libitum*).

2. Experimental design

The study was designed to find the impact of the therapeutic use of different doses of chloroquine on progression of malaria pathogenesis using a model of *Plasmodium berghei* ANKA infected ICR mice. To achieve this, it was mandatory to pass through the sequential processes of the parasite maintenance, establishment of the infection's models, the *in vivo* screening of the anti-malarial drugs and monitoring of the disease progression.

All the experiments were performed as per rules and guidelines of the Institutional Animal Care and Use Committee (IACUC) of the University Putra Malaysia. The protocol was approved by the committee [Ref # UPM/ IACUC-R044/2016].

3. Parasite maintenance

3.1. Animals infection

Initially, a group of mice was inoculated I.P with 0.2 ml of the thawed cryopreserved parasites and the parasitemia was monitored daily using the well-known Giemsa stained thin blood film technique (Ameri, 2010). The animals were sacrificed, and their blood was collected by a cardiac puncture under ketamine xylazine anesthesia for further passaging or cryopreservation once their parasitemia reached a level of 35%; the parasitemia threshold for passaging and cryopreservation. Then, the animal's carcasses were disposed of, according to rules and guidelines of the ethical committee (Basir, Rahiman *et al.*, 2012).

3.2. Parasite cryopreservation

The collected blood (Section 2.3.1) was mixed with the Alservers anticoagulant buffer at a ratio of 1:3 (blood/ buffer) (Basir *et al.*, 2012) and kept in tightly stoppered cryo-vials and kept at -80°C.

3.3. Parasites passaging

For passaging, standard inoculums of 5×10^7 /ml of PRBCs (parasitized RBCs) were prepared through mixing the collected blood with N/S at [(1: X-1 (infected blood / N/S)) where in X=parasitemia of the infected blood]. Then, the inoculums were injected to ICR mice; weighing 17–20g, and the animals were monitored daily for the parasitemia progression till reaching the level of the exsanguination.

4. Establishment of *Plasmodium berghei* ANKA infected ICR mice model and design of the study

The study was designed based on a preliminary study wherein 10 ICR mice were injected with 0.2 ml of an inoculum containing 1×10^7 PRBCs I.P. Then, they were monitored during the subsequent days for the parasite growth, cardinal signs of the disease and the hematology parameters till the animal's death. The cardinal signs appeared once the parasitemia reached to the threshold of

20–30%. Meanwhile, the sudden mortality was observed at a parasitemia level > 60% as only 30% of the mice experienced that before reaching this limit. Besides, there has been an inter-individual variation in the time required to reach the mentioned thresholds (data are not shown).

Accordingly, the experiment was designed to inject chloroquine once the parasitemia reached the threshold of 20–30% (experimental initiation point) and to terminate the study when the level exceeded the 60% (the experimental termination point) to avoid this source of error or loss of the animals by the sudden mortality.

5. Establishment of the positive control group (reference comparator group)

The positive control group was established as in the preliminary study but the monitoring continued till reaching the experimental termination point. The required period to achieve this point was set as a criterion for the animal's survival which was determined using the well-known Kaplan-Meir's estimator. Furthermore, the animals were left for 10 days in case of having a complete eradication of the parasites. At the termination point, the animals were exsanguinated after collecting their blood by cardiac puncture under xylazine/ ketamine anesthesia. The organs were removed, washed with PBS (Phosphate buffer saline (pH=7.4)), weighed and kept in formalin for the histology study. The remaining carcass was wrapped to be disposed of as per the guidelines of the ethical committee.

6. Dose response curve of chloroquine and its impact on the disease progression

The dose response curve of chloroquine against the used model was determined using Rane's protocol for the *in vivo* screening of the anti-plasmodium drugs with modifications wherein the drugs are given after establishment of the infection (Tarkang *et al.*, 2014; Upegui *et al.*, 2014).

Briefly, five different groups (n=10) were appropriated, viz; CQT1, CQT5, CQT10, CQT15, and CQT20, and were treated with 1, 5, 10, 15 and 20 mg/kg of chloroquine I.P respectively, and the animals were monitored subsequently as in the positive control (Sections 2.5).

A stock solution of 10 mg/ml of chloroquine was used to prepare working solutions at the required concentrations to deliver the mentioned doses. The final volume was adjusted such that it did not exceed the maximum injectable volume of the I.P injection of the drugs to the mice (0.1 ml for each 10 g of the body weight) as recommended by the Canadian Council on animal care (CCAC) guidelines (Ernest *et al.*, 1993).

7. Sample size calculation

The minimum acceptable sample size was calculated using Lambert's power model (Kadam and Bhalero, 2010) depending on the change in the parasitemia during the preliminary study after the injecting the parasites at the experimental initiation point. The parasitemia jumped from 22.14 ± 1.12 to 38.34 ± 1.34 on the next day (Figure 1). The model showed that five is the minimum statistically acceptable number for this study. But, in this study, ten mice were allocated for each group to secure having more than five samples for the biochemistry and the histology study.

8. Animals monitoring

The tail blood was collected daily to monitor the parasites growth and changes in the hematology parameters. The former was determined using the well-known Giemsa stained thin blood smears technique (Basir *et al.*, 2012) while the BC-5200 Hematology Analyzer was used for the WBCs and RBCs counts (Mindray, Nanshan, Shenzhen, China).

Besides, the cardinal signs of the disease (body weight, body temperature, piloerection, locomotor activity and dark urine) were monitored. The body weight was measured

using Shimadzu (UX4200H) top pan animal balance to the nearest 0.1g. The colonic temperature was measured using BIOSEB (BIO9882) rectal thermometer with a probe inserted 1.5 cm post the anal sphincter into the colon of handheld mice. Meanwhile, the behavioral changes were observed and graded using an arbitrary 4-point scale (0=absence, 1=mild, 2=moderate and 3=severe). On the other hand, a binomial scale (0=absent, 1=present) was adopted to evaluate the incidence of dark urine. The monitoring continued until the mice died spontaneously.

The blood collected blood samples were used to measure serum level of the liver enzymes (SGOT, SGPT, ALT and GGT), total bilirubin and serum proteins to assess the liver functions, each of the serum urea, creatinine for the renal function and each of Na⁺, K⁺, Ca⁺⁺, PO₄⁻² and Cl⁻ to assess the impact on the electrolytes homeostasis.

After dissecting the animals, the organs were collected, blotted in Whatman filter paper, monitored for the morphology changes, weighed to calculate their index and kept in formalin before exposing them to the sequential steps of the histology slide procession and staining.

9. Statistical analysis

One-way ANOVA was used to test for the significance of the difference between the groups using the SPSS software/ version 21. Meanwhile, all the histology changes were scored by a pathologist using the ordinal method of the histology slides scoring. A score range of 0-5 was given for each event to represent absence, very mild, mild, moderate, severe and very severe, respectively. They were analyzed using the non-parametric Kruskal Wallis test followed by the Man Whitney test to compare between the groups.

On the other hand, the survival profile of the all the groups was determined using the Kaplan Mier's estimator paired with log-rank (Mantel-Cox) and Gehan-Beslow-Wilcoxon test for the pairwise comparisons. The test does not merely measure the equity of the survival of the populations but it also gives a weight to the incidence of the early death and the survival time.

RESULTS

1. Parasitemia progression and animal's survival in chloroquine treated and untreated *Plasmodium berghei* infected ICR mice

The study showed a progressive increase in the hematology and the clinical parameters within the positive control and in a parasitemia dependent manner. Its survival profile revealed that only 3 out of 10 animals died before reaching the experimental termination point (Figure 1).

Chloroquine administration produced a dose dependent decline in the parasitemia, such that, a complete eradication was achieved for the individuals of the CQT20 group and for 70% of CQT15. Nevertheless, a sub-therapeutic effect was obtained at 5 and 10 mg/kg wherein the parasite recrudescence was observed. The parasitemia growth profile at 1 mg/kg was comparable to that of the control (Figure 1, Table 1). The survival study showed that chloroquine treatment at 15 and 20 mg/kg produced a statistically significant survival curve as compared to the positive control as per log-rank (Mantel-Cox) test ($P < 0.05$) while Gehan-Breslow-Wilcoxon test failed to show any statistical significance among the groups.

1.1. Clinical signs of the disease

The positive control mice experienced a progressive decline in the body weight (Figure 1) along with the incidence of piloerection, and lethargy effective from the 3rd day post-infection up to the end of the study. Dark urine was observed only during the late stages, although its incidence was inconsistent in all the animals. Despite the decline in the parasitemia after chloroquine treatment, the mice continued experiencing a prominent loss in the body weight (Figure 1) and the mentioned signs during the first few days post-treatment (data are not shown). Later on, the symptoms were settled down for the CQT20 group but turned stronger for the recrudescence groups (CQT5 and CQT10 groups). Meanwhile, the symptoms were comparable to that of the positive control at 1 mg/kg.

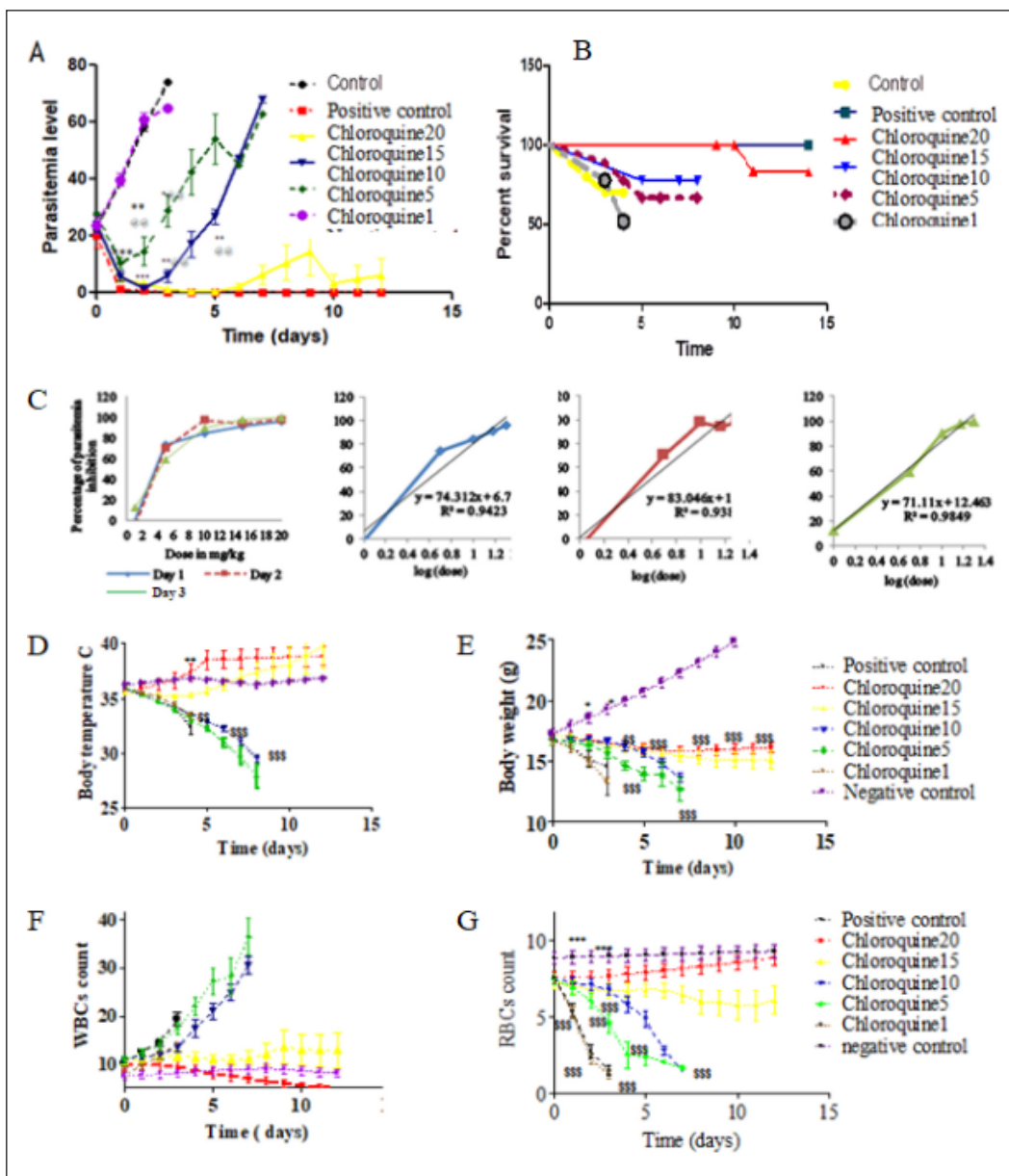


Figure 1. Parasitaemia progression, dose response curve and survival profile after chloroquine treatment, body temperature, body weight and hematology parameters after chloroquine treatment. A- Parasitemia progression in the positive control and the chloroquine treated groups. B- Survival profile of the chloroquine treated and untreated *Plasmodium berghei* ANKA infected ICR mice. Using Kaplan Meir estimator. C- The dose-response curves for the therapeutic effect of chloroquine during the subsequent three days after the treatment. Meanwhile the changes in the body temperature, body weight, WBCs count (C), RBC count in the chloroquine treated and untreated groups were represented by curves D, E and F and G respectively. The results were expressed as mean \pm SEM (*, ** and ***) and (§, §§ and §§§) signify statistically significant difference as compared to the positive and negative controls ($P < 0.05$, $P < 0.01$ and $P < 0.001$ respectively).

Table 1. Therapeutic potency of chloroquine during the first 3 days post infection

Day	ED _{50T}	ED _{90T}	ED _{99T}
1	3.82	13.20	17.45
2	3.85	11.70	15.02
3	3.33	12.23	16.39

ED_{50T}, ED_{90T} and ED_{99T} refer to the effective therapeutic dose required to inhibit the parasite growth by 50, 90 and 99%, respectively in mg/kg.

1.2. Hematology parameters in chloroquine treated and untreated *Plasmodium berghei* ANKA infected ICR mice

A progressive and consistent leukocytosis and anemia were observed in the positive control, and in a parasitemia dependent. This picture continued after chloroquine therapy during the first few days. The changes settled down for CQT20, worsened for CQT5 and CQT10 and were similar to that of the positive control at the lowest dose (Figure 1).

1.1. Biochemistry parameters in chloroquine treated and untreated *Plasmodium berghei* ANKA infected ICR mice

A moderate renal and hepatic dysfunction was observed in the infected groups at the end of the study. They were stronger in the recrudescence groups but resolved for the CQT20. Similarly, a mild hyponatremia and hypocalcaemia, hyperkalaemia, hyperchloremia and hyperphosphatemia were observed in the positive control but resolved after having a complete parasite eradication (CQT20) but turned stronger in the mentioned recrudescence groups. (Figure 1). Meanwhile, they were comparable to that of the control for the CQT1 (Table 2).

1.2. Histology and necroscopic changes in chloroquine treated and untreated *Plasmodium berghei* ANKA infected ICR mice

1.2.1. Necroscopic changes

Red discoloration and organomegaly were the main necroscopy features of organs of the infected mice (positive control group).

They were highly prominent in the liver and spleen, moderate in kidneys and lungs, minimal in the brain and absent in the heart (Table 2). The changes were stronger and at the utmost extent the recrudescence groups (especially the changes in liver and spleen). The changes persisted at a comparable extent to that of the control for CQT20 and CQT1 (Table 2).

1.2.2. Effect on liver

The infected positive control mice experienced prominent changes within the hepatic sinusoids, hepatic cord and portal triad. The cord showed mild loss of the hexagonal architecture, mild hepatocytes shrinkage and very few foci of vacuolar or nuclear degeneration. Furthermore, mild to moderate sinusoidal dilation and tissue hemozoin deposition were seen as well. The sinusoids were predominated with hypertrophied and hyper-proliferated Kupffer cells as well as the infiltrated lymphocytes. Meanwhile, the portal triads of the hepatic lobules experienced mild congestion of the hepatic veins and arteries along with perivascular cuffing of leucocytes around the portal triads (Figure 2).

Comparable changes to that of the positive control were observed at 1 mg/kg. Meanwhile, the changes were stronger in the recrudescence groups wherein foci of necrosis and nuclear degeneration were observed. At 15 and 20 mg/kg, less hemozoin deposition, hepatic cord shrinkage and damage as compared PC was observed but the degree of sinusoidal congestion, lymphocytes infiltration, Kupffer cells hyperplasia and WBCs cuffing within the portal tract were higher (Figure 2).

1.2.3. Effect on spleen

Spleens of the positive control showed higher cellularity and abundance of the pluripotential hematopoietic cells as compared to negative control. The white pulp was enlarged and showed loss of the germinal center details and the distinctive demarcation with the red pulp (Figure 3). The changes were comparable to the control in CQT1 and were more obvious for the recrudescence groups wherein the hyper-

Table 2. Biochemistry parameters

Parameter	Negative control	Positive control	CQT20	CQT15	CQT10	CQT5	CQT1
Renal function parameters							
Creatinine in $\mu\text{mol/l}$	98.5 \pm 3.8 ^{bbb}	256.4 \pm 7.2 ^{aaa}	113.3 \pm 2.9 ^{bbb}	122.3 \pm 5.9 ^b	288.2 \pm 8.1 ^{aa}	292.3 \pm 9.3 ^{aaa}	283.1 \pm 6.9 ^{aaa}
Urea in mmol/l	22.2 \pm 1.3 ^{bb}	41.3 \pm 4.6 ^{aa}	26.3 \pm 1.2 ^{bb}	29.3 \pm 1.6 ^{bb}	46.2 \pm 2.4 ^{aa}	44.2 \pm 2.4 ^{aaa}	37.2 \pm 2.3 ^{aaa}
Uric acid in mmol/l	188.3 \pm 3.1 ^{bb}	411.8 \pm 4.6 ^{aa}	212.3 \pm 3.1 ^{bb}	219.5 \pm 3.1 ^b	511.5 \pm 6.2 ^a	563 \pm 8.3 ^a	398.4 \pm 3.9
Electrolytes							
Sodium	144.3 \pm 2.3	126.2 \pm 1.9	138.6 \pm 2.6	133.6 \pm 2.3	112.5 \pm 2.3	118.6 \pm 2.6	127.6 \pm 2.2
Potassium	7.3 \pm 0.55	9.1 \pm 0.42	8.3 \pm 0.71	8.5 \pm 0.81	9.7 \pm 0.65	10.2 \pm 0.76	9.1 \pm 0.72
Calcium	12.6 \pm 1.11 ^b	8.7 \pm 0.72 ^a	12.1 \pm 0.93	11.3 \pm 0.87	8.3 \pm 0.72 ^a	8.1 \pm 0.71 ^a	9.4 \pm 0.81
Phosphate	9.1 \pm 1.2	13.4 \pm 1.7	10.1 \pm 1.2	10.9 \pm 1.3	15.8 \pm 1.6	16.1 \pm 1.3	12.9 \pm 1.2
Chlorine	112.3 \pm 3.4	132.6 \pm 4.1	121.5 \pm 3.7	124.2 \pm 4.1	137.5 \pm 3.8	141.2 \pm 3.1	131.5 \pm 4.3
Liver function tests							
SGOT (I.U/l)	35 \pm 1.4	93.5 \pm 2.4 ^{aa}	81.3 \pm 2.6 ^{aaa}	75.6 \pm 1.9 ^{aa}	198 \pm 4.6 ^{aaab}	211.8 \pm 3.8 ^{aaabbb}	105.3 \pm 2.6 ^{aaa}
SGPT (I.U/l)	68.2 \pm 2.7	182 \pm 4.8 ^{aaa}	153.2 \pm 3.9 ^{aa}	142.6 \pm 3.9 ^{aa}	377 \pm 4.1 ^{aaabbb}	369.2 \pm 4.8 ^{aaabbb}	196.3 \pm 4.3 ^{aaa}
Total bilirubin	0.33 \pm 0.009 ^{bbb}	1.12 \pm 0.013 ^{aaa}	0.43 \pm 0.011 ^{bba}	0.46 \pm 0.016 ^{bbb}	2.23 \pm 0.01 ^{aaab}	2.46 \pm 0.017 ^{aaabbb}	1.23 \pm 0.019 ^{aaa}
Globulin (mg/dl)	1.83 \pm 0.025 ^{bbb}	5.62 \pm 0.037 ^{aaa}	3.32 \pm 0.029 ^{ab}	3.44 \pm 0.041 ^{bb}	8.93 \pm 0.04 ^{aaabbb}	9.25 \pm 0.047 ^{aaabbb}	5.32 \pm 0.039 ^{aaa}
Albumin (mg/dl)	3.8 \pm 0.032 ^{bb}	2.8 \pm 0.043 ^{aa}	3.15 \pm 0.038	3.21 \pm 0.039	1.85 \pm 0.06 ^{aaabbb}	1.75 \pm 0.062 ^{aaabbb}	2.7 \pm 0.039 ^{aa}
Globulin/ albumin	0.47 \pm 0.04 ^b	2.01 \pm 0.05 ^{aa}	1.07 \pm 0.041	1.08 \pm 0.039	4.82 \pm 0.05 ^{bbb}	5.23 \pm 0.071	1.97 \pm 0.041
γ -GGT (I.U/l)	5.3 \pm 0.42 ^b	13.2 \pm 0.62 ^a	7.2 \pm 0.48	6.9 \pm 0.51	21.6 \pm 0.85 ^{ab}	23.6 \pm 1.06 ^{ab}	15.2 \pm 0.71 ^a
ALP (I.U/l)	75.3 \pm 2.9 ^{bb}	213.6 \pm 4.3 ^{aa}	162 \pm 3.2 ^a	164 \pm 4.7 ^a	433.5 \pm 10.2 ^{aaabbb}	523.3 \pm 12.3 ^{aaabbb}	219.6 \pm 6.3 ^{aa}
Organs indices							
Liver	4.21 \pm 0.23 ^{bbb}	8.74 \pm 0.89 ^{aaa}	9.12 \pm 1.03 ^{aaa}	8.65 \pm 1.12 ^{aaa}	11.9 \pm 0.54 ^{aaa}	12.2 \pm 0.61 ^{aaab}	8.32 \pm 0.78 ^{aa}
Kidneys	1.31 \pm 0.072 ^b	1.82 \pm 0.091 ^a	1.76 \pm 0.083	1.75 \pm 0.09	2.06 \pm 0.10 ^{aa}	2.12 \pm 0.17	1.69 \pm 0.097
Brain	1.52 \pm 0.08	1.76 \pm 0.11	1.69 \pm 0.093	2.02 \pm 0.11	2.29 \pm 0.12	2.34 \pm 0.13	1.81 \pm 0.12
Spleen	0.41 \pm 0.032 ^{bbb}	1.35 \pm 0.052 ^{aaa}	1.30 \pm 0.043 ^{aaa}	1.33 \pm 0.062 ^{aaa}	2.22 \pm 0.09 ^{aaabbb}	2.31 \pm 0.08 ^{aaabbb}	1.41 \pm 0.045 ^{aaa}
Lungs	0.91 \pm 0.022	1.62 \pm 0.051 ^a	1.41 \pm 0.033	1.53 \pm 0.051	1.72 \pm 0.061	1.75 \pm 0.042	1.56 \pm 0.061

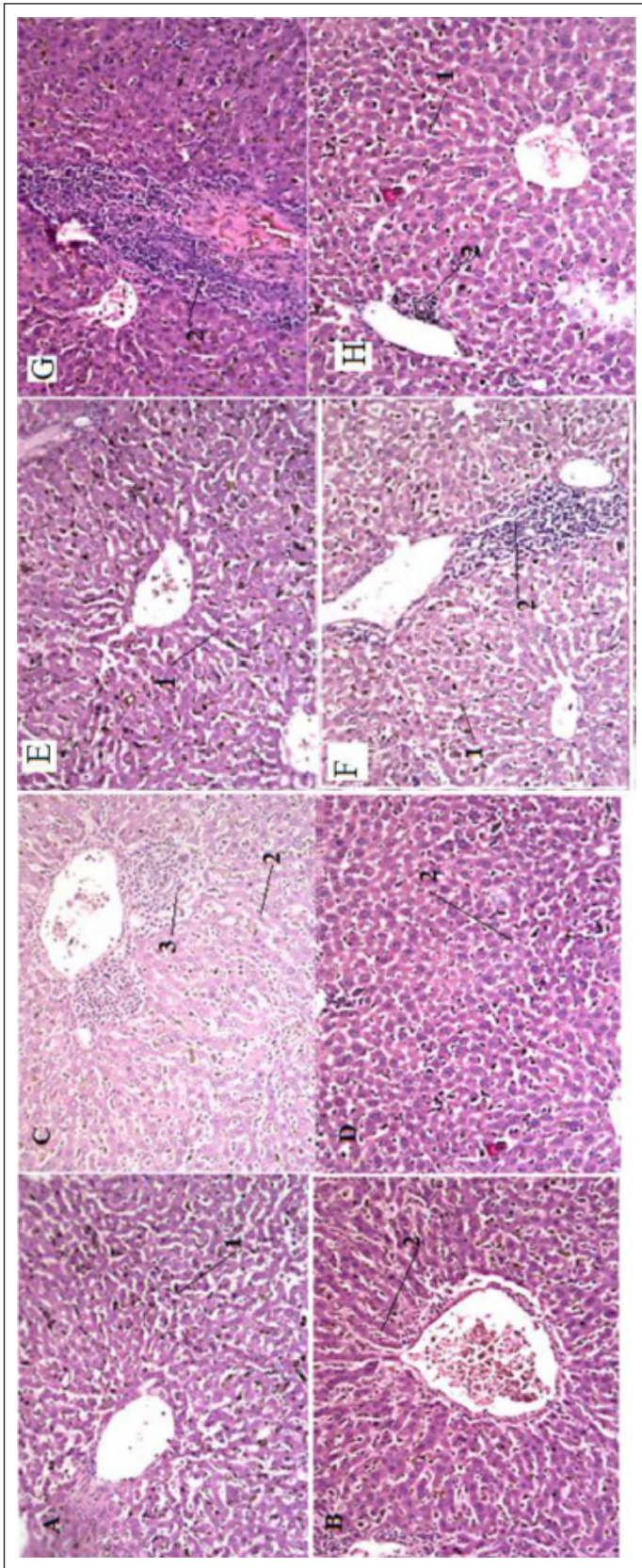


Figure 2. Liver histology.

Snapshots of liver histology slides obtained from Chloroquine treated and untreated *Plasmodium berghei* ANKA infected and uninfected mice at 20 and 40X. A, B, C and D belong to slides obtained from PC, CQT5, CQT10 and CQT20 at 20X respectively. Meanwhile, E, F, G and H represents slides obtained from the same groups but at 40X. The slide shows that the sinusoidal dilation (1) was comparable in the treated and untreated mice. Lymphocytes infiltration and Kupffer cells hyper-proliferation were more obvious in the chloroquine treated mice as compared to the untreated mice. Hematoxylin cuffing (3) was seen in all the slides (brown deposits) except for those treated with the highest dose of chloroquine. Leucocytes cuffing (2) was seen in all the slides and reached to its upmost level in CQT10.

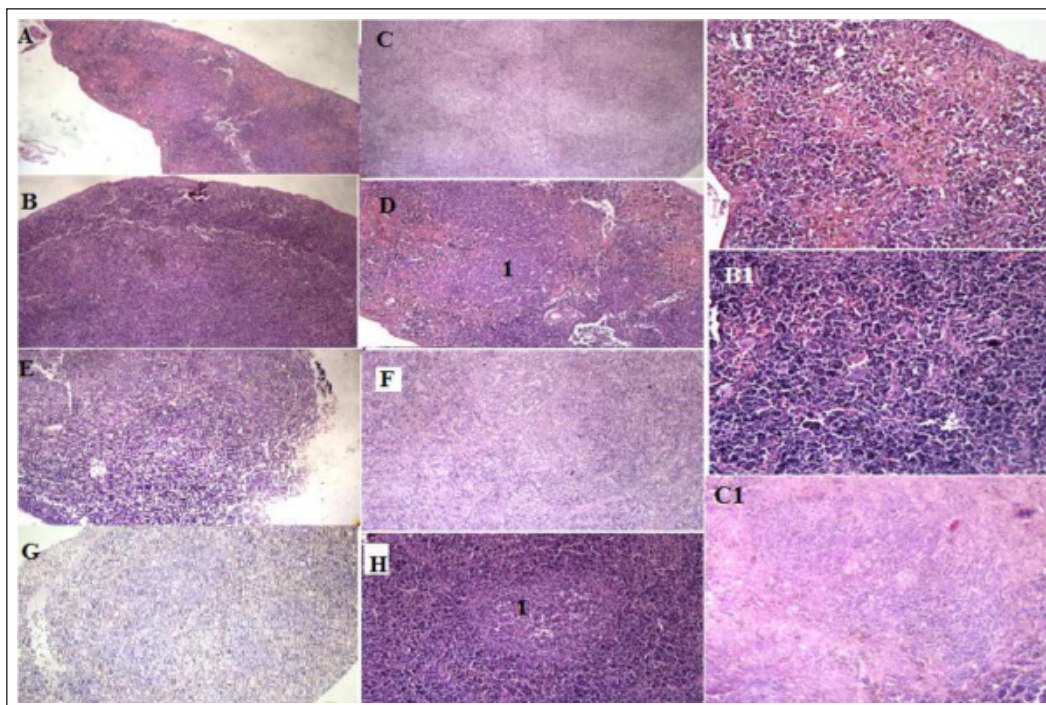


Figure 3. Spleen histology.

Snapshot image of spleen histology slides obtained from Chloroquine treated and untreated *Plasmodium berghei* ANKA infected mice at 4, 10 and 20X. A, B, C and D belong to slides obtained from PC, CQT5, CQT10 and CQT20 at 4X respectively. Meanwhile, E, F, G and H were obtained from the same groups at 10X. Furthermore, A1, B1, C1 belong to slides obtained from PC, recrudescence groups and those showed complete parasite eradication (CQT20). Hypercellularity was seen in the white and red pulps of all the spleens and were more marked in those obtained from mice that experienced parasite recrudescence. Hemozoin deposition (brown black deposits) was obtained for PC and all the chloroquine treated mice except for CQT20 wherein the deposition was minimal. Furthermore, more hematopoietic stem cells were observed in CQT5 and CQT10 groups as compared to the other groups. All the slides showed e hypercellularity and enlargement of the white pulp along with loss of the demarcation between both white and red pulps. These features were prominently higher in the Chloroquine treated group and reached to its upmost level for CQT10. Meanwhile, they were less in the CQT20 treated groups.

cellularity, hemozoin deposition and white pulp enlargement were more. The slides showed also a complete loss of the demarcation of the marginal zone between white and red pulps and higher abundance of the extra-medullary hematopoietic cells (pro-generator myeloid cells).

1.2.4. Effect on kidneys

Kidneys of the positive control showed cortical and medullary changes. The cortical changes were mild to moderate and characterized by glomerular hypercellularity and congestion, mesangial cells hyperproliferation, mild to moderate tubular degenerative changes. The renal interstitial

spaces showed very mild depositions of hemozoin along with mild lymphocytes infiltration. Generally, the kidneys of the positive control group are less affected by the infection as compared to the other organs, as; liver and spleen (Figure 4).

Similar histology changes were observed after chloroquine treatment with the highest intensity in the recrudescence groups. Besides, unique events were observed in the later groups, such as the incidence of the DCT (Distal Convolved Tubules) ectasia with protein cast, acute renal tubular necrosis with nuclear sloughing and damage in the renal medulla with medullary vascular congestion. Nonetheless, at 20 mg/kg, the

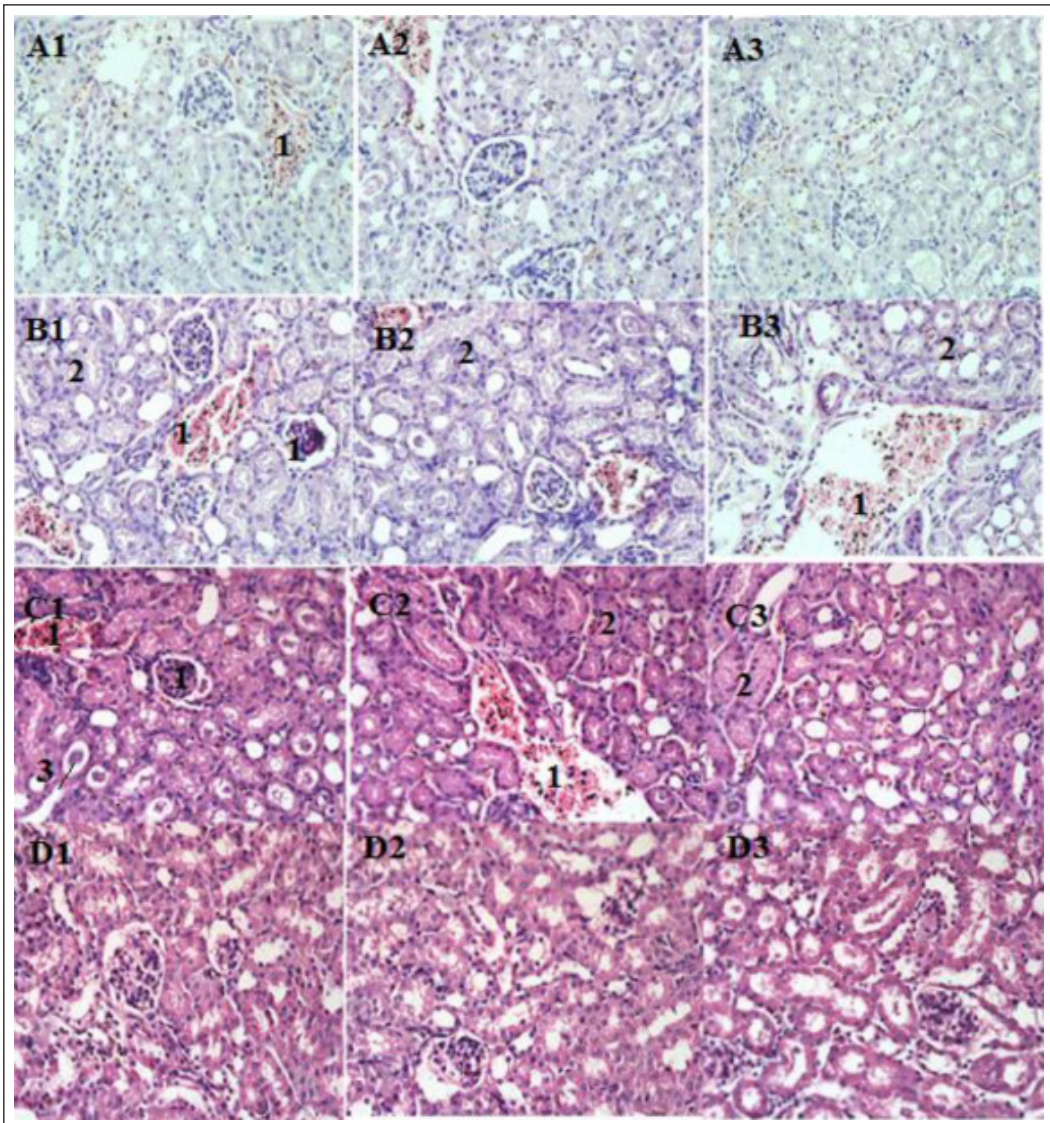


Figure 4. Kidney histology.

Snapshot image of kidney histology slides obtained from Chloroquine treated and untreated *Plasmodium berghei* ANKA infected mice at 40 X. A, B, C and D belong to slides obtained from PC, CQT5, CQT10 and CQT20 at 40X respectively. All of them showed vascular and glomerular congestion (1), tubular damage (2) and DCT ectasia by protein cast (3). These changes were slightly more severe in CQT10 as compared to the others. CQT20 showed similar changes except for the parasite sequestration.

changes were milder than that of the positive control without having any form of the hemozoin deposition or intravascular sequestration of the PRBCs (Figure 4).

1.2.5. Effect on lungs

Lungs of the positive control showed mild architectural distortion, thickening of the alveolar septa, pulmonary edema, hemorr-

hage, hemozoin deposition and hyperproliferation of the alveolar macrophage. But a few slides showed few foci of hyalinization (Figure 5). Beside these features, the recrudescence groups also experienced alveolar hemorrhage, pulmonary necrosis, emphysema and pulmonary edema. The changes were exceptionally stronger in CQT5 (Figure 5).

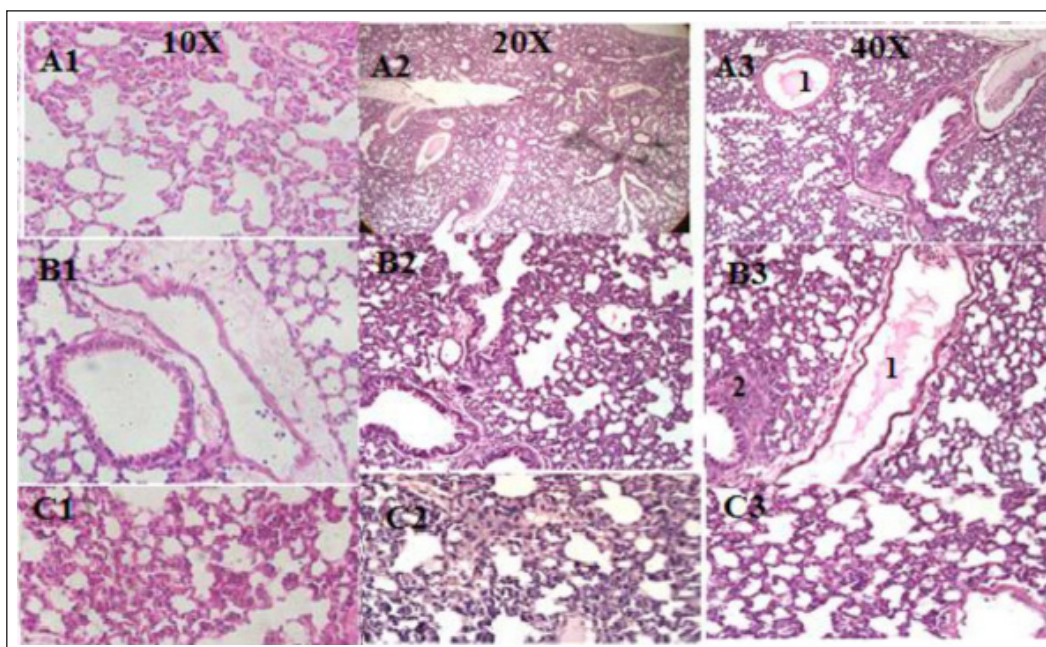


Figure 5. Lungs histology.

Snapshot image of lungs histology slides obtained from Chloroquine treated and untreated *Plasmodium berghei* ANKA infected mice at 10, 20 and 40 X. A1, B1, C1 belong to slides obtained from the positive control, Chloroquine treated infected mice and showed recrudesence and those treated after full recovery at 10X. A2, B2 and C2 as well as A3, B3 and C3 were taken from the same groups at 20 and 40X respectively. Thickening of the alveolar wall and its congestion with the polymorphonuclear cells was a characteristic trait for all the slides. The phenomenon was at its upmost level for those that showed recrudesence especially for CQT10 and lower for the other groups. Pulmonary oedema was seen in mice that experienced recrudesence and in the positive control (1). Hyalinization was seen in slides of the mice lungs that showed recrudesence (2).

As what we have seen in kidneys, both of the hemozoin deposition and PRBCs sequestration were disappeared at 20 mg/kg but the other histology features remained at a comparable extent to that of the positive control. Similarly, the changes at 1 mg/kg were comparable to that of the positive control.

1.2.6. Effect on the brain

Few histology changes were observed in brains of the infected mice. Neurons of the cerebral cortex were normal within the molecular and granular layers. Nevertheless, mild hyper-cellularity; characterized by astrocytosis and oligodendrocytes hyper-proliferation, was observed. Furthermore, some foci of vascular congestion and mild petechial hemorrhage were seen in most of the slides and few of them showed intravascular sequestration of PRBCs.

(Figure 6). It is noteworthy that the brain index of the positive control was slightly and insignificantly different as compared to that of the positive control ($P < 0.05$).

In spite of the insignificant difference in the brain index between the positive control and the recrudesence groups. Stronger histology features were observed in the later groups as compared to the positive control. They showed more microglial hyper-proliferation; which was very mild in PC as well as brain hemorrhage and mild neuronal damage. Both of the brain hemorrhage and neuronal damage appeared as a new feature in the recrudesence groups and were absent in the positive control group. The hypercellularity persisted after giving chloroquine at 20 mg/kg but there was no any foci of vascular congestion, hemorrhage or parasites sequestration (Figure 6).

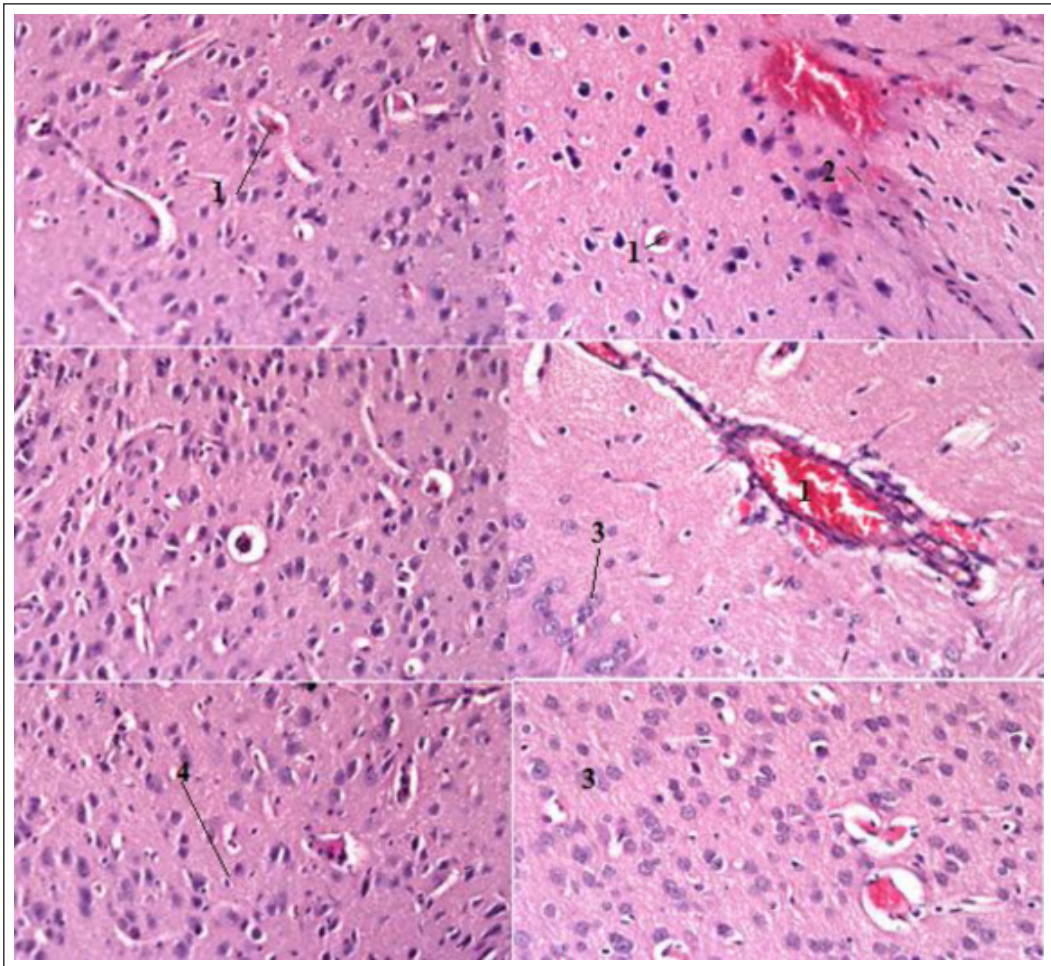


Figure 6. Brain histology.

Images of histology slides obtained from the brain of Chloroquine treated *Plasmodium berghei* ANKA infected ICR mice model after parasite recrudescence at 40X. The slides revealed prominent hyper-cellularity with a prominent increase in astrocytes, oligodendrocytes and microglia along with foci of vascular congestion (1), focal cerebral haemorrhage (2), astrocytosis (3), and microglia hyperproliferation (4).

DISCUSSION

1. *Plasmodium berghei* infected ICR model

Unfortunately, Dissemination of chloroquine resistance amongst different strains of *Plasmodium falciparum* has compromised its importance as a potential. Furthermore, the pharmacokinetic characters of chloroquine made it difficult to maintain its serum level at the therapeutic level. This study aimed at determining the impact of treatment failure of chloroquine on the disease progression (Schroeder and Gerber, 2014). A model of *Plasmodium berghei*

ANKA- infected-mice was used in the study as it is inaccessible to use the *Plasmodium falciparum* infected human model due to ethical issues (Stevenson *et al.*, 2010; Langhorne *et al.*, 2011).

Plasmodium berghei cycle takes 24 hours to accomplish one intra-erythrocytic cycle and release a new batch of the infectious merozoites. Each schizont produces 6-12 merozoites (Langhorne *et al.*, 2011) suggesting that the actual number of the PRBCs may duplicate by this factor after each cycle. Nevertheless, in our experiment, the number was duplicated by 4.8, 2.3 and 1.2 for the positive control within the first three

days post-infection respectively. This can be ascribed to the host derived immune response or to the infection induced pathogenic changes (Basir *et al.*, 2012); that makes the milieu less favorable for the parasites to survive. Furthermore, the aptitude of the merozoites to invade new RBCs may be compromised by other factors, such as the relative preference of the parasite to the reticulocytes; which are more abundant in the early stage of the infection and disappear along with its progression (Srivastava *et al.*, 2015), loss of the RBCs integrity due to the infection induced biochemical changes as well as their tendency to perform rosetting (Ribacke *et al.*, 2013). But anyway, counting the parasites in the peripheral blood may underestimate the actual picture of the parasitemia as a population of the parasites may sequester in the microvasculature of spleen, kidneys, liver, lungs and the cerebrum as seen in the histology study (Ling *et al.*, 2008).

During the establishment of the model, there has been a slight inter-individual variation in the rate of the parasitemia development among the infected mice, and this may affect the reliability of the study. To overcome this, we opted to set and experimental initiation point at a specific threshold which was (20-30%) regardless of the time that the mice took to get that level of the infection.

The hematology changes and the observed clinical changes in the positive control can be ascribed to the infection-induced cytokine shock (Modiano *et al.*, 2001). The immune response starts recruitment of the histiocytes (splenic macrophages and Kupffer cells) to encounter the infected RBCs. Then, they transform to potential immune-blasts that impart in mediation of the cytokine shock (Modiano *et al.*, 2001; Basir *et al.*, 2012).

The clinical changes included cachexia, lethargy, loss of locomotor activity, piloerection and loss of body weight (Basir *et al.*, 2012). Cachexia is attributed to the interference of the cytokines with the cellular building and nutrients influx to the muscles resulting in loss of the lean tissues and the bodyweight (Molanouri-Shamsi *et al.*, 2014).

On the other hand, the behavioral changes can be also ascribed to the decline in the neuronal functions which may occur after having the observed metabolic disarrays. (Jens *et al.*, 1985). For instance, the incidence of the mild hyperkalemia or the accumulation of the nitrogenous waste products.

The incidence of anemia can be ascribed to the parasites ingestion of hemoglobin as a sole source of amino acids or induction of the RBCs rupture by the merozoites that leave the cells at the end of the cycle or accumulation of heme; the toxic waste product of hemoglobin ingestion, that leads to oxidative stress and enhancement of the RBCs membrane breakdown (Olivier *et al.*, 2014). Generally, anemia is associated with reticulocytosis; which occurs due to the overproduction erythropoietin from the Juxtaglomerular apparatus of the DCTs. Erythropoietin is a glycoprotein; released in response to low oxygen tension to trigger the red bone marrow to produce more RBCs. In most anemic cases, a dys-erythropoietic reaction evolves and the immature reticulocytes erupt into the circulation (Rotz *et al.*, 2016). But this phenomenon was absent in the infected mice due to the incidence of the cytokine shock which directs the red bone marrow activity toward WBCs production or the insensitivity of the erythroblasts to the erythropoietin after down-regulation of the transferrin receptors expression (Hoffmann *et al.*, 1999).

It worth to note that in malaria both of the cytokine shock and anemia act cooperatively to precipitate the infection-induced clinical signs and symptoms. They change the biochemical nature of the body resulting in loss of the functional characteristic of the nervous system.

Besides, the histology changes in the brain can be linked to the incidence of the behavioral changes. The slides showed hyper-proliferation of the oligodendrocytes and the astrocytes. The former produces the myelin sheath that wraps and insulates the neuronal axons and expedites the transfer of the electric signals within the neuronal network. Meanwhile, the astrocytes are octopus-like cells endowed with plenty of perivascular feet that aid in shuffling of

nutrients from the cerebral micro-vessels into neurons. Incidence of the vascular congestion within the cerebral cortex is an indicative of a disturbed cerebral micro-vascular circulation that incurs as a normal consequence of the intravascular parasite sequestration or incidence of the cytokine shock (Roerink *et al.*, 2017).

As an intracellular pathogen, plasmodium induces predominance of the Th1 cytokine profile that is characterized by the high release of the main proinflammatory cytokines, such as; of TNF- α , INF- γ and IL-1. This was confirmed in our experiment through results of the peripheral WBCs count, spleen and liver indices which were increased significantly along with the progression of the disease. Both of spleen and liver are parts of the reticuloendothelial system which impart significantly in the progression of the inflammatory reactions. On the other hand, their histopathological changes were characterized by hypercellularity, vascular congestion, lymphocytes infiltration and local tissues macrophage hyperproliferation (Kupffer cells and splenic macrophages) (Basir *et al.*, 2012).

The study also showed that the infection was associated with vascular, degenerative, or inflammatory changes. The vascular events can be attributed to the intravascular sequestration of the PRBCs or to the cytokine-shock-induced-inflammatory-reaction. Meanwhile, the degenerative changes are attributed to the incidence of the hypoxia or over-activation of macrophages phagocytosis which results in seeping of hydrolytic enzymes and oxidative stress markers into the surrounding milieu (Basir *et al.*, 2012).

It worth to note that the parasite invasion induces membranous remodeling in the infected RBCs; which is characterized by overexpression of EMP-1 (Electron Membrane Protein). EMP-1 mediates for PRBCs adhesion to the endothelium through binding to a complementary adhesion molecule present on the endothelial surface; vascular ICAM (Intra-Cellular Adhesion Molecule). Furthermore, this process induces PRBCs rosetting and creation of sludge that occlude blood circulation (Ribacke *et al.*, 2013).

Overall, PRBCs membrane remodeling can be set as one of the causative factors that lead to vascular occlusion and enhancement of malaria induced degenerative changes.

The observed stronger inflammatory changes in the liver and spleen (organs of the reticuloendothelial system); that came in tandem with the leukocytosis, gives a notion that the disease pathogenicity is more related to the incidence of the cytokine shock rather than to the clog of the blood vessels by the sequestered parasites (De Souza *et al.*, 2010). The notion was also evidenced by the biochemistry results that showed a higher globulin/ albumin ratio which suggests activation of the antibody mediated response (Cooke and Coppel, 1995). Although, in this occasion, the animals experienced also glomerular changes which may lead to further loss of albumin that also impart in rising up this ratio. Absence of the histology changes in the heart and their presence in the other organs also suggest the insignificance of the vascular changes and predominance of the host derived immune reaction in our model as their occurrence is expected in the coronary circulation. The heart is less affected histologically by the cytokine shock as unlike other organs, it is not endowed with a great deal of WBCs burden (Cooke and Coppel, 1995).

Once the macrophages engulf the parasitized RBCs, they start releasing a bunch of hydrolytic enzymes that break down the parasite components leaving hemozoin; which is an indigestible waste product of the parasite metabolic activity. This is followed by a secondary response characterized by a surge of the cellular respiratory oxidative mechanism and generation of oxygen free radicals (Fazalul Rahiman *et al.*, 2013). Seeping of the free radicals into the surrounding tissue may impart in the mediation of the plasmodium induced degenerative changes. Hemozoin deposition was seen in the stroma of the liver, spleen and kidneys. Previously, it was thought that its deposition might enhance the macrophages phagocytic activity and seeping out of the hydrolytic enzymes (Buffet *et al.*, 2011).

Clogging of blood vessels by the sequestered parasites lessens blood and oxygen perfusion, decreases ATP generation. This explains the observed vacuolar degeneration and the few necrotic changes that we observed in some of the slide (Vidale *et al.*, 2017).

Prominence of the oligodendrocytes and astrocytes in the brain without having any neuronal damage or microglial hyperproliferation suggests induction of a compensatory mechanism toward the infection induced stress.

The mild hepatic dysfunction in the infected mice can be ascribed to the phagocytic activity of the Kupfer cells or diminution in the blood perfusion. They came in tandem with the results of the liver function tests. The results suggest a loss of the hepatocytes membrane integrity as indicated by leakage of the main hepatic transaminases AST (Aspartate Transaminase) and ALT (Alanine transaminase), which were multiplied by about 3 times as compared to the uninfected control.

The study also revealed a prominent but insignificant increase in leakage of the bile canalicular enzymes ALP (alkaline phosphatase) and γ -GGT (γ -glutamyl transferase enzymes). This increase can be ascribed to the prominent mild perivascular cuffing of the leucocytes around the portal triads as seen in the histology study. The leucocytes activity is associated with leakage of its hydrolytic enzymes that may adversely affect the integrity of the bile canalicular cells resulting in leakage of these enzymes into the extracellular compartment (Sharma and Prasad *et al.*, 2014). The biliary changes were confirmed by the prominent increase in the level of the conjugated bilirubin.

The results also suggest a mild loss in the detoxification power of the hepatocytes as indicated by the mild elevation of the plasma level of the unconjugated bilirubin (indirect bilirubin). This indicates that the mice had experienced a condition of mixed hepatic and post hepatic hyperbilirubinemia and the defect in the bile canalicular duct might have played a major rule in pre-

cipitation of the hyperbilirubinemia (Sugawara *et al.*, 2012).

Kidneys of the infected mice showed glomerular and tubular changes. The formers can be ascribed to the infection-induced-vascular-changes and to the mesangial hyperproliferation; that occurs as a response to cytokine shock (Ibraheem *et al.*, 2012). Overstimulation of the phagocytic activity of the renal mesangial cells and deposition of heme and hemozoin within the infected kidneys might have imparted in raising the incidence of glomerulonephritis. It worth to note that the overactivation of podocytes in response to the intra-glomerular is the culprit behind the observed thickening of the glomerular basement membrane (Ibraheem *et al.*, 2014). Meanwhile, the tubular changes can be ascribed to the higher intra-renal oxidative stress in response to the inflammatory reaction or deposition of the parasites' waste products. Interstitial nephritis was noticed due to the deposition of hemozoin, heme, and PRBCs. While the medullary changes can be ascribed to the distortion in the vascular flow and the infection-induced-oxidative-stress. At this stage, dark urine was observed as one of the clinical symptoms. This came in tandem with hemozoin deposition within the renal tissue and a high incidence of RBCs hemolysis. RBCs hemolysis causes a release of a copious quantity of heme derivatives which may appear as black pigments during urination.

The condition was also characterized by disturbance of the electrolytes balance (Na^+ , K^+ , Ca^{++} , Cl^- and HPO_4^-). Although, the kidney plays a major role in their control but their level can be affected by other organs. The study revealed an incidence of a very mild and insignificant hyponatremia; which is attributed to the loss of the renal tubular function. This observation can be linked to results of previous studies that pointed out to the coincidence of the hypotensive shock along with malaria (Miller *et al.*, 2013). presence of the tubular damage within the medulla along with the vascular congestion of the vasa recti suggests a defect in the counter multiplication mechanism within the

loop of Henle which contributes to water and sodium reabsorption from the collecting tubules into the renal medulla. Although it is not expected that this decline plays an important role in the mediation of malaria induced hypotension as it was minimal and insignificant. The increase in the flow of the inflammatory mediators during the cytokine shock may have a major contribution to the incidence of malaria associated hypotension (Basir *et al.*, 2012).

Results of potassium level revealed prominent hyperkalemia. It is very important to note that the increased serum potassium is quietly related to the incidence of hemolysis during blood sampling. Care was taken during blood collection and serum level of potassium in the hemolyzed samples was ignored. But in spite of that, the level was higher in the infected group, and this can be ascribed to the infection-induced-RBCs-rupture, the degenerative and necrotic changes in the liver and kidneys or the lactic acidosis; which is one of the manifestations of malaria. It triggers leakage of potassium from the intracellular toward the extracellular compartments (Brand *et al.*, 2016).

Lactic acidosis can be attributed to the anaerobic fermentation of glucose by the parasite or due to the ischemic changes induced by the intravascular sequestration of the PRBCs (Basir *et al.*, 2012). These changes were observed obviously in the histology slides of liver and kidneys of the infected animals. Furthermore, the changes in the lung's histology suggests a deterioration in the exchange of the respiratory gases and retention of carbon dioxide. Moreover, loss of the hemoglobin can be set as another factor that deteriorates the blood buffer capacity and enhances the acidotic changes.

The observed hyponatremia can be attributed to the incidence of the hyperkalemia; which limits the incidence of the former through triggering the DCT in kidneys to reabsorb more sodium in the replacement of potassium. But anyway, renal loss of potassium is expected due to the incidence of the mild renal tubular damage (Brand *et al.*, 2016).

The serum electrolyte profile also showed a decline in calcium level. This can be ascribed to a decrease in the food uptake or the intestinal absorption of calcium or an increase in its excretion through the renal pathway. Renal reabsorption of calcium is quietly related to vitamin D homeostasis. Vitamin D activation requires intact hepatocytes and renal mesangial cells. So any defect in these sites results in loss of vitamin D activation (Hollis and Wagner 2013).

The decline in serum calcium was mild, and the infected group showed a heteroscedastic standard deviation as compared to the negative control. The changes in the protein profile is expected to produce a prominent effect on calcium level as its level is affected by 0.8 mg/dl with every 1 g/dl change in the albumin level and by 0.12 mg/dl for every 1 g/dl change in globulin (Kurbel, 2011).

Besides, this change was accompanied by a prominent hyperphosphatemia whose incidence can be attributed to leakage of the intracellular phosphate after having the parasite induced RBCs rupture and cellular damage in the affected organs. Furthermore, incidence of hypocalcemia triggers release of the parathyroid hormone; which increases phosphate level through induction of the hydroxyapatite resorption inhibition of phosphate reabsorption in the PCT. Moreover, the parathyroid hormone induces renal excretion of the released phosphate through inhibition of its reabsorption in the PCT and inhibits calcium excretion through triggering its reabsorption in the DCT. Nevertheless, this effect may be outweighed by the incidence of renal failure that results in reduction of the amount of phosphate that filters into in the tubules due to the diminution in the glomerular filtration rate (Kurbel, 2011; Mishra, 2013).

Moreover, mild hypochloremia was observed in the infected mice; which can be ascribed to the loss of the tubular function that lead to chlorine leakage with urine or to the presence of the acidosis that triggers the renal compensatory mechanism to

excrete more chlorine in the replacement of bicarbonate (Eisenhut 2006).

The DCT showed a deposition of an extensive amounts of protein cast. This phenomenon occurs as a normal outcome of the glomerulonephritis; which is characterized by the reduced ability of the glomeruli to retain the low gram molecular weight proteins. Along with their passage, they slough the mucopolysaccharides that line up the tubular epithelium resulting in the intratubular deposition of what is called the protein cast (Ibraheem *et al.*, 2012).

2. Therapeutic use of chloroquine

The dose-response curve of the growth inhibitory effect of chloroquine showed that its inhibitory effect persisted during the subsequent days suggesting a consistent bioavailability during this period or other biologically active metabolites were produced.

This notion coincides with the information about chloroquine pharmacokinetics as its half-life is relatively long (about 2-3 days in rodents). Furthermore, it tends to accumulate in various body compartments and it has a high binding affinity to plasma (60%) and tissue proteins, such as; melanin. This makes its level in the lean body mass and the central nervous system reaches to 300-700 and 10-30 times that in plasma respectively. on this occasion, the lean body mass acts as a depot from where, chloroquine is released continuously to compensate for the amounts eliminated by the liver or kidneys (Ono *et al.*, 2003, Pang, 2003). The high binding capacity of chloroquine to melanin makes the uveal tract of eyes and skin as the most attractive sites for its accumulation (Schroeder and Gerber, 2014). The long half-life of chloroquine is not attributed only to its accumulation in the lean body mass but also to its slow elimination. Its hydrophilic characters make its excretion to be exclusively throughout the kidneys. Although the pharmacokinetic studies revealed that chloroquine is also affected by the hepatic metabolism. Chloroquine metabolism results in the creation of pharmacologically active metabolites, such

as; des-ethyl chloroquine which also imparts in protraction of its pharmacological effect inside the body. Chloroquine possesses structural characters; characterized by ubiquity of several hydroxyl substitutions that makes it a target for plenty of drugs metabolizing enzymes.

The urinary excretion of chloroquine constitutes about 40-70% of the ingested drug. It is affected by pH such that urinary acidification increases chloroquine ionization and reduces its renal tubular reabsorption resulting in higher chloroquine excretion. (Pereira *et al.*, 2016). On the other hand, hepatic elimination occurs via metabolic processes, such as; oxidative deamination, side chain elimination and N-oxidation pathways using CYP2C8, CYP2A4, and CYP2D6 as cofactors. The main metabolites are; N-des-ethyl-chloroquine and N-bis-des-ethyl-chloroquine from the oxidative deamination pathway, 7-chloro-4-aminoquinoline from the side-chain elimination pathway and chloroquine-N-oxide and chloroquine dioxide from the N-oxidation pathway. N-des-ethyl-chloroquine is the main metabolite. It possesses a potential anti plasmodium effect and its $T_{1/2}$ is relatively longer than that of chloroquine. Its blood level gives is highly correlated with chloroquine uptake (Projean *et al.*, 2003). Chloroquine has a long $T_{0.5}$ reaching to 3-6 days in humans and 2-3 days in rats. Meanwhile, its tissue $T_{0.5}$ is about 300 hours (McLachlan *et al.*, 1993). All of these factors might have also contributed to the risk of having chloroquine at the subtherapeutic threshold.

This study was concerned about how do the pathogenic events change along with complete or incomplete chloroquine therapy. In spite of its prominent growth inhibitory effect, chloroquine treatment failed to affect the changes in the cardinal signs of the disease and WBCs count as they continued in a manner comparable to that of the positive control. This can be attributed to the persistence of the molecular machinery mechanisms related to the overstimulation of the host immune response. Previous studies have highlighted the immune suppressive

effects of chloroquine (Nishimura *et al.*, 1998). But this action was not observed in our experiment and this may be due to the insufficiency of the chloroquine level for conferring this action. But unlike the other parameters, the change in the RBCs count was a dose-dependent manner as the infection induced RBCs hemolysis is quietly related to the parasite burden rather than the machinery of the immune system (Basir *et al.*, 2012).

Three different histology patterns were observed after treating the mice with different doses of chloroquine. One of them was comparable to that of the control, and was observed in CQT1. Stronger changes were observed in the recrudescence groups (CQT5 and CQT10) although their final parasitemia was similar to that of the untreated control at the experimental termination point (section 3.5). The slides showed that most of them were related to overactivation of the immune system. But they showed more parasite sequestration and hemozoin deposition. This suggests that the total parasite burden in the recrudescence groups was higher than that of the control in spite of having a comparable level of peripheral parasitemia (Lehnhardt and Kemper *et al.*, 2011; Miller *et al.*, 2013).

The discrepancy between the actual parasite burden and the peripheral parasitemia is expected due to the screening method as the used Giemsa stained smear technique does not reflect the total parasite burden within the body. Other techniques that rely on determining the blood level of the parasites derived antigens may give a clearer picture. This discrepancy is expected to be higher in the recrudescence group as per the histology results showed higher hemozoin deposition and PRBCs sequestration.

The higher PRBCs sequestration can be attributed to the stronger host immune response during recrudescence. Overstimulation of the immune reaction was deduced from the hematology results that showed an exceptional increase in WBCs count. Furthermore, the biochemistry showed higher globulin/albumin ratio as compared to that obtained during the early infection. Adhesion of the parasitized RBCs to the vascular endothelium is closely

related to the cytokine shock as the released cytokines trigger expression of more endothelial adhesion molecules; that mediate the infected cells sequestration (Cooke and Coppel, 1995; Cooke *et al.*, 1995; De Souza, 2010).

Slides of the recrudescence groups showed unique histology features; absent in the positive control. For instance; hemorrhage in the brain, higher incidence of the acute tubular necrosis and deposition of casts in the DCT of the kidneys or the incidence of necrotic damage in the liver and the lungs. This reflects the steadier and faster progression of the pathogenic events after exposure to recrudescence.

CONCLUSION

All in all, in spite of the observed protraction in the animal's survival at the sub-therapeutic dose of chloroquine; the individuals can experience more fastidious clinical or the histopathologic changes within parasitemia thresholds comparable to that of the untreated control.

Complete or partial eradication of the parasitemia does not resolve the case completely during the subsequent days of the treatment as the individuals continue experiencing changes related to the overstimulation of the immune system.

Future recommendations

The study recommends pursuing further investigations regarding the pharmacokinetic behavior of chloroquine during the active infection of plasmodium and further elucidation of how chloroquine therapeutic treatment affects the molecular machinery of the infection induced immune stimulation.

Conflict of interest

All the authors declare that there is no conflict of interest related to the publication of this manuscript.

Acknowledgment. University Putra Malaysia is acknowledged for providing the facilities and the grant to accomplish this research.

REFERENCES

- Ameri, M. (2010). Laboratory diagnosis of malaria in nonhuman primates. *Veterinary and Clinical Pathology* **39**: 5-19.
- Basir, R., Rahiman, S., Hasballah, K., Chong, W.C., Talib, H. & Yam, M.F. (2012). *Plasmodium berghei* ANKA Infection in ICR Mice as a Model of Cerebral Malaria. *Iranian Journal of Parasitology* **7**: 62-74.
- Basir, R., Hasballah, K., Jabbarzare, M., Gam, L.H., AbdulMajid, A.M., Yam, M.F., Moklas, M.A., Othman, F., Che-Norma, M.T., Zalinah, A., Mahmud, R. & Abdullah, W.O. (2012). Modulation of interleukin-18 release produced positive outcomes on parasitemia development and cytokines production during malaria in mice. *Tropical Biomedicine* **29**: 405-421.
- Brand, N.R., Opoka, R.O., Hamre, K.E. & John, C.C. (2016). Differing Causes of Lactic Acidosis and Deep Breathing in Cerebral Malaria and Severe Malarial Anemia May Explain Differences in Acidosis-Related Mortality. *PLoS ONE* **11**: e0163728.
- Buffet, P.A., Safeukui, I., Deplaine, G., Brousse, V., Prendki, V., Thellier, M., Turner, G.D. & Mercereau-Puijalon, O. (2011). The pathogenesis of *Plasmodium falciparum* malaria in humans: insights from splenic physiology. *Blood* **117**: 381-392.
- Cooke, B.M. & Coppel, R.L. (1995). Cytoadhesion and falciparum malaria: going with the flow. *Parasitology Today* **11**: 282-287.
- Cooke, B.M., Morris-Jones, S., Greenwood, B.M. & Nash, G.B. (1995). Mechanisms of cyto-adhesion of flowing, parasitized red blood cells from Gambian children with falciparum malaria. *American Journal of Tropical and Medical Hygiene* **53**: 29-35.
- De Souza, J.B., Riley, E.M. & Couper, K.N. (2010). Cerebral malaria: why experimental murine models are required to understand the pathogenesis of disease. *Parasitology* **137**: 755-772.
- Eisenhut, M. (2006). Causes and effects of hyperchloremic acidosis. *Critical Care* **10**: 413-413.
- Ernest, D., Olfert, D.V., Brenda, M., Cross, D.V. & AnnMcWilliam, A. (1993). *Guide to the care and use of experimental animals*, Ottawa, Canadian Council on Animal Care.
- Fazalul-Rahiman, S.S., Basir, R., Talib, H., Tie, T.H., Chuah, Y.K., Jabbarzare, M., Chong, W.C., MohdYusoff, M.A., Nordin, N., Yam, M.F., Abdullah, W.O. & Abdul-Majid, R. (2013). Interleukin-27 exhibited anti-inflammatory activity during *Plasmodium berghei* infection in mice. *Tropical Biomedicine* **30**: 663-680.
- Hoffmann, J.J. & Pennings, J.M. (1999). Pseudo-reticulocytosis as a result of malaria parasites. *Clinical Laboratory Hematology* **21**: 257-260.
- Hollis, B.W. & Wagner, C.L. (2013). The Role of the Parent Compound Vitamin D with Respect to Metabolism and Function: Why Clinical Dose Intervals Can Affect Clinical Outcomes. *Journal of Clinical Endocrinology and Metabolism* **98**: 4619-4628.
- Ibraheem, Z.O., Abdul Majeed, R., Mohd. Noor, S., Mohd. Sedik, H. & Basir, R. (2014). Role of Different Pfcrt and Pfmdr-1 Mutations in Conferring Resistance to Antimalaria Drugs in *Plasmodium falciparum*. *Malaria Research and Treatment* **2014**: 17.
- Ibraheem, Z.O., Basir, R., Aljobory, A.K., Ibrahim, O.E., Alsumaidae, A. & Yam, M.F. (2014). Impact of Gentamicin Coadministration along with High Fructose Feeding on Progression of Renal Failure and Metabolic Syndrome in Sprague-Dawley Rats. *BioMed Research International* **2014**: 823879.
- Ibraheem, Z.O., Sattar, M.A., Abdullah, N.A., Rathore, H.A. & Johns, E.J. (2012). Effect of high saturated free fatty acids feeding on progression of renal failure in rat model of experimental nephrotoxicity. *Bosnian Journal of Basic Medical Science* **12**: 26-32.
- Jens, H., Henriksen, J.H., Ring-Larsen, H. & Christensen, N.J. (1985). Sympathetic nervous activity in cirrhosis. *Journal of Hepatology* **1**: 55-65.

- Kadam, P. & Bhalerao, S. (2010). Sample size calculation. *International Journal of Ayurveda Research* **1**: 55-57.
- Kurbel, S. (2011). Donnan effect on chloride ion distribution as a determinant of body fluid composition that allows action potentials to spread via fast sodium channels. *Theoretical Biology & Medical Modelling* **8**: 16-16.
- Langhorne, J., Buffet, P., Galinski, M., Good, M., Harty, J. & Leroy, D. (2011). The relevance of non-human primate and rodent malaria models for humans. *Malaria Journal* **10**: 23-23. doi: 10.1186/1475-2875-10-23
- Lehnhardt, A. & Kemper, M.J. (2011). Pathogenesis, diagnosis and management of hyperkalemia. *Pediatric Nephrology* (Berlin, Germany). *Pediatric Nephrology* **26**: 377-384.
- Ling, S., Nheu, L., Dai, A., Guo, Z. & Komesaroff, P. (2008). Effects of four medicinal herbs on human vascular endothelial cells in culture. *International Journal of Cardiology* **128**: 350-358.
- McLachlan, A., Tett, S., Day, R. & Cutler, D., (1993). Interpretation of chloroquine pharmacokinetic data. *European Journal of Clinical Pharmacology* **44**: 407-410.
- Miller, L.H., Ackerman, H.C., Su, X. & Wellems, T.E. (2013). Malaria biology and disease pathogenesis: insights for new treatments. *Nature Medicine* **19**: 156-167.
- Mishra, S. (2013). Malaria precipitated hypercalcemia and related complications. *The Pharma Innovation Journal* **2**: 162-168.
- Modiano, D., Sirima, B.S., Konate, A., Sanou, I. & Sawadogo, A. (2001). Leukocytosis in severe malaria. *Transactions of Royal Society of Tropical Medicine and Hygiene* **95**: 175-176.
- Molanaouri-Shamsi, M., Hassan, Z.H., Gharakhanlou, R., Quinn, L.S., Azadmanesh, K., Baghersad, L., Isanejad, A. & Mahdavi, M. (2014). Expression of interleukin-15 and inflammatory cytokines in skeletal muscles of STZ-induced diabetic rats: effect of resistance exercise training. *Endocrine* **46**: 60-69.
- Nishimura, M., Hidaka, N., Akaza, T., Tadokoro, K. & Juji, T. (1998). Immunosuppressive effects of chloroquine: potential effectiveness for treatment of post-transfusion graft-versus-host disease. *Transfusion Medicine* **8**: 209-214.
- Olivier, M., Van-Den-Ham, K., Shio, M.T., Kassa, F.A. & Fougeray, S. (2014). Malarial Pigment Hemozoin and the Innate Inflammatory Response. *Frontiers in Immunology* **5**: 10-20.
- Ono, C., Yamada, M. & Tanaka, M. (2003). Absorption, distribution and excretion of ¹⁴C-chloroquine after single oral administration in albino and pigmented rats: binding characteristics of chloroquine-related radioactivity to melanin *in-vivo*. *Journal of Pharmacy and Pharmacology* **55**: 1647-1654.
- Pang, K.S. (2003). Modeling of intestinal drug absorption: roles of transporters and metabolic enzymes for the Gillette Review Series). *Drug Metabolism and Disposition: The Biological Fate of Chemicals* **31**: 1507-1519.
- Pereira, D., Daher, A., Zanini, G., Maia, I., Fonseca, L., Pitta, L., Ruffato, R., Marchesini, P. & Fontes, C.J. (2016). Safety, efficacy and pharmacokinetic evaluations of a new coated chloroquine tablet in a single-arm open-label non-comparative trial in Brazil: a step towards a user-friendly malaria vivax treatment. *Malaria Journal* **15**: 477. doi: 10.1186/s12936-016-1530-0
- Projean, D., Baune, B., Farinotti, R., Flinois, J.P., Baune, P., Taburet, A.M. & Ducharme, J. (2003). *In vitro* metabolism of chloroquine: identification of CYP2C8, CYP3A4, and CYP2D6 as the main isoforms catalyzing N-desethylchloroquine formation. *Drug Metabolism and Disposition* **31**: 748-754.
- Ribacke, U., Moll, K., Albrecht, L., Ahmed-Ismail, H., Normark, J., Flaberg, E., Szekely, L., Hultenby, K., Persson, K.E., Egwang, T.G. & Wahlgren, M. (2013). Improved *in vitro* culture of *Plasmodium falciparum* permits establishment of clinical isolates with preserved multiplication, invasion and

- rosetting phenotypes. *PLoS ONE* **22**: e69781.
- Roerink, M.E., Van-der-Schaaf, M.E., Dinarello, C.A., Knoop, H. & van der Meer, J.W. (2017). Interleukin-1 as a mediator of fatigue in disease: a narrative review. *Journal of Neuro-inflammation* **14**: 16 doi: 10.1186/s12974-017-0796-7
- Rotz, S.J., Ann-O'riordan, M., Kim, C., Langer, N., Cruz, C., Schilz, R., Lance, C. & Little, J.A. (2016). Nocturnal hemoglobin desaturation is associated with reticulocytosis in adults with sickle cell disease and is independent of obstructive sleep apnea. *American Journal of Hematology* **91**: E355-6. doi: 10.1002/ajh.24432.
- Sharma, U. & Prasad, R. (2014). Alkaline phosphatase: an overview. *Indian Journal of Clinical Biochemistry* **29**(3): 269-278.
- Schroeder, R.L. & Gerber, J.P. (2014). Chloroquine and hydroxychloroquine binding to melanin: Some possible consequences for pathologies. *Toxicology Reports* **1**: 963-968.
- Srivastava, A., Creek, D.J., Evans, K.J., De-Souza, D., Schofield, L., Müller, S., Barrett, M.P., McConville, M.J. & Waters, A.P. (2015). Host Reticulocytes Provide Metabolic Reservoirs That Can Be Exploited by Malaria Parasites. *PLoS Pathogens* **11**: e1004882.
- Stevenson, M.M., Gros, P., Olivier, M., Fortin, A. & Serghides, L. (2010). Cerebral malaria: human versus mouse studies. *Trends in Parasitology* **26**: 274-275. doi: 10.1016/j.pt.2010.03.008.
- Sugawara, K., Nakayama, N. & Mochida, S. (2012). Acute liver failure in Japan: definition, classification, and prediction of the outcome. *Journal of Gastroenterology* **47**: 849-861. doi: 10.1007/s00535-012-0624-x.
- Tarkang, P.A., Okalebo, F.A., Ayong, L.S., Agbor, G.A. & Guantai, A.N. (2014). Antimalarial activity of a polyherbal product (Nefang) during early and established plasmodium infection in rodent models. *Malaria Journal* **13**: 456.
- Upegui, Y., Robledo, S.M., Gil-Romero, J.F., Quiñones, W., Archbold, R., Torres, F., Escobar, G., Nariño, B. & Echeverri, F. (2015). *In vivo* Antimalarial Activity of α -Mangostin and the New Xanthone δ -Mangostin. *Phytotherapy Research* **29**: 1195-1201.
- Vidale, S., Consoli, A., Arnaboldi, M. & Consoli, D. (2017). Post- ischemic Inflammation in Acute Stroke. *Journal of Clinical Neurology* **13**: 1-9.
- Wang, X., Li, H., Zheng, A., Yang, L., Liu, J., Chen, C., Tang, Y., Zou, X., Li, Y., Long, J., Liu, J., Zhang, Y. & Feng, Z. (2014). Mitochondrial dysfunction-associated OPA1 cleavage contributes to muscle degeneration: preventative effect of hydroxy-tyrosol acetate. *Cell Death and Disease* **5**: e1521. doi: 10.1038/cddis.2014.473.